Asymmetric Planetary Nebulae III
ASP Conference Series, Vol. XXX, 2004
M. Meixner, J. Kastner, B. Balick and N. Soker eds.

Evidence for bipolar jets in late stages of AGB winds

D. Vinković[1], M. Elitzur

Department of Physics & Astronomy, University of Kentucky, Lexington, KY 40506-0055

K.-H. Hofmann, G. Weigelt

Max-Planck-Institut für Radioastronomie, Auf dem Hügel 69, 53121 Bonn, Germany

Abstract. Bipolar expansion at various stages of evolution has been recently observed in a number of AGB stars. The expansion is driven by bipolar jets that emerge late in the evolution of AGB winds. The wind traps the jets, resulting in an expanding, elongated cocoon. Eventually the jets break-out from the confining spherical wind, as recently observed in W43A. This source displays the most advanced evolutionary stage of jets in AGB winds. The earliest example is IRC+10011, where the asymmetry is revealed in high-resolution near-IR imaging. In this source the jets turned on only $\sim$ 200 years ago, while the spherical wind is $\sim$ 4000 years old.

The premise that asymmetric planetary nebulae (PNe) evolve from spherically symmetric Asymptotic Giant Branch (AGB) winds raises one of the most intriguing questions of stellar astrophysics: when and how does the stellar wind break its spherical symmetry? Since many proto-planetary nebulae (PPNe) show distinct large-scale asymmetries (e.g. Su, Hrivnak & Kwok 2001, Sahai 2002), the symmetry breaking process has to operate already during the late stages of AGB evolution. This implies that AGB winds are not always spherical. Indeed, in recent years, high-resolution imaging has yielded conclusive evidence of asymmetry for several AGB objects (V Hya: Plez & Lambert 1994, Sahai et al. 2003; X Her: Kahane & Jura 1996; IRC+10011: Hofmann et al. 2001; IRC+10216: Weigelt et al. 1998 & 2002, Haniff & Buscher 1998, Skinner et al. 1998, Osterbart et al. 2000; RV Boo: Bergman et al. 2000, Biller et al. 2003; CIT6: Lindqvist et al. 2000, Monnier et al. 2000, Schmidt et al. 2002). There have been suggestions that asymmetries could be even prevalent in AGB winds (Plez & Lambert 1994, Kahane at al. 1997).

1. Jet-driven asymmetry evolution in AGB stars

Concurrently, an increasing number of jet and jet-like features has been identified in various PNe and PPNe, prompting a suggestion that jets are also responsible

[1]School of Natural Sciences, Institute for Advanced Study, Princeton, NJ 08540

for symmetry breaking in AGB winds (Sahai & Trauger 1998). The strongest evidence for jets comes from maser observations, including proper motion measurements, of both the fast collimated jets and the slow spherical wind (e.g., IRAS 16342-3814: Sahai et al. 1999; K3-35: Miranda et al. 2001; Hen 3-1475: Riera et al. 2003; IRAS 22036+5306: Sahai et al. 2003). Probably the youngest display of such a configuration of masers is the AGB star W43A (Imai et al. 2002). Considering that these jets are detected when they already break out from the confinement of a slow high density AGB wind, there has to exist an earlier instance of jet-evolution when only a small expanding cocoon is detectable (Scheuer 1974).

If large scale bipolar jet-cavities were to be carved out from the AGB wind of PPNe, as demonstrated in IRAS 16342-3814, then the cocoon expansion has to operate already during the AGB phase. Thus the aforementioned asymmetric AGB objects should provide glimpses of the cocoon expansion. The direct kinematic evidence of this process exists only for V Hya and W43A, where expansion velocities are measured. In the other objects, asymmetries revealed in imaging observations fit into this scenario.

The youngest example of a jet-cocoon in AGB stars, as we argue in section 2.2., exists in IRC+10011. A more advanced stage of cocoon evolution is present in the prototype C-rich star IRC+10216. Its cocoon is of a similar size, but the asymmetry is more pronounced and evident even in the K-band, unlike IRC+10011 where only the J-band image shows clear asymmetry. The C-rich star V Hya provides an example that is further along in evolution. Recent CO observations by Sahai et al. (2003) show a morphology of a bipolar outflow with velocities of 100–150 km s^{-1} breaking from the confinement of the high-density region of the slowly expanding AGB wind. A similar structure has been found in the O-rich star X Her, with a spherical wind of 2.5 km s^{-1} and two symmetrically displaced 10 km s^{-1} components, likely to be the red and blue shifted cones of a weakly collimated bipolar flow. An even more evolved system is the C-rich star CIT6, where a bipolar asymmetry dominates the image both in molecular line mapping and in HST-NICMOS imaging.

These examples show that a bipolar asymmetry, most probably created by collimated outflows, appears during the final stages of AGB mass outflow. This represents the first instance of symmetry breaking in the evolution from AGB to planetary nebula. It is still not clear, however, what physical process drives these jets. Diversity in their properties could lead toward diversity in geometrical and physical properties of the bipolar asymmetry. When the AGB phase ends, a mixture of various processes emerges, such as multiple jets and fast winds. Their interaction with the AGB circumstellar asymmetries leads to the myriad of complex structures found in PPN and PN sources.

2. IRC+10011: the youngest example of jets in AGB stars?

The oxygen-rich star IRC+10011 (= IRAS 01037+1219 = CIT3 = WXPsc) is one of the most extreme infrared AGB objects. It is surrounded by an optically thick dusty shell formed by a large mass loss rate of $\sim 10^{-5} M_{\odot} yr^{-1}$. The shell expansion velocity of $\sim$ 20 km s^{-1} has been measured in OH maser and CO lines. This source served as the prototype for the first detailed models of AGB

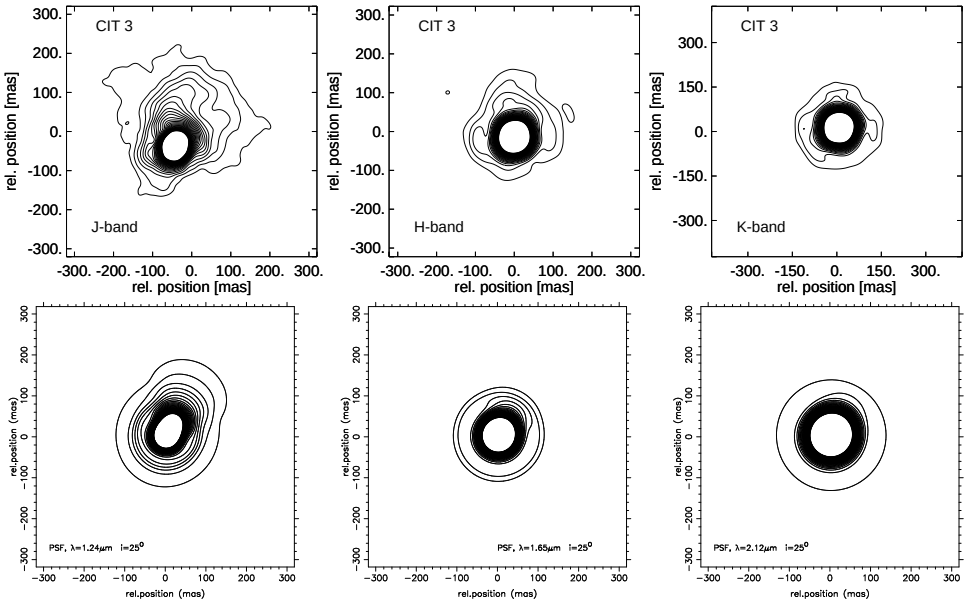

Figure 1. Upper row: Near infrared images of IRC+10011 in the J- (1.24μm), H- (1.65μm) and K'-band (2.12μm) with respective resolutions of 48 mas, 56 mas and 73 mas (H01). Lower row: Theoretical images based on 2D radiative transfer convolved with the instrumental PSF of H01. Contours are plotted from 1.5% to 29.5% of the peak brightness in steps of 1%. The transition from scattered light dominance in the J-band to thermal dust emission in the K'-band creates a sudden disappearance of the image asymmetry (Figure 2). The bright fan-shaped structure is scattered light escaping through the polar cone carved out by the jet.

winds by Goldreich & Scoville (1976) and of the OH maser emission from OH/IR stars by Elitzur, Goldreich, & Scoville (1976). The sphericity of its dusty wind had been considered secure. The recent discovery by Hofmann et al. (2001; H01 hereafter) of distinct asymmetries in its envelope was, therefore, a surprise. They obtained the first near infrared bispectrum speckle-interferometry observations of this source with a resolution of tens of AU (Figure 1, upper row). While the H- and K'-band images appear almost spherically symmetric, the J-band shows a clear asymmetry.

2.1. 2D radiative transfer modeling

These images impose strong constrains on the circumstellar dust density distribution in the inner regions. It can be easily shown that scattering by a $1/r^p$ dust density distribution produces a $1/r^{p+1}$ brightness profile. Since the J-band image at 1.24 μm is dominated by dust scattering, the following geometry was deduced directly from the image: along the polar axis, the dust density declines as $1/r^{0.5}$, while the rest of the dusty wind has the typical $1/r^2$ density profile (Figure 2, left). Without good observational constraints on the large scale

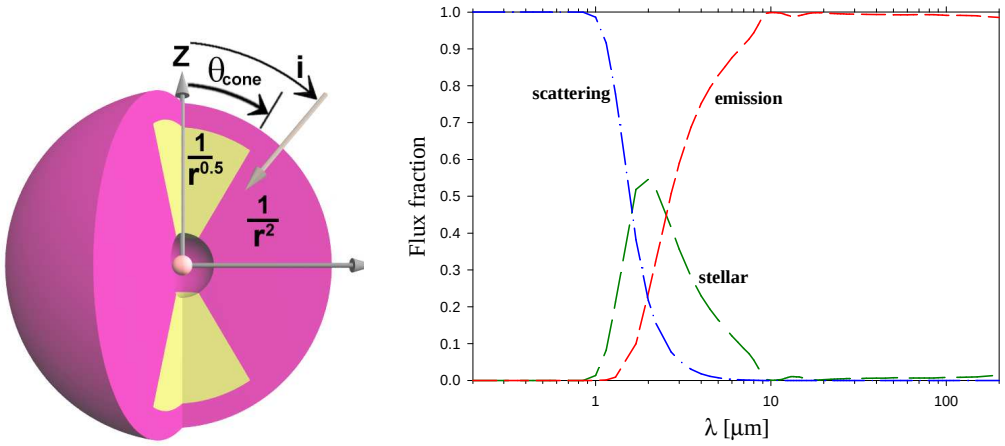

Figure 2. Left: Sketch of the 2D model for the circumstellar dusty shell around IRC+10011. Two polar cones with half-opening angle θ_{cone} and a $1/r^{0.5}$ density profile are imbedded in a spherical wind with the standard $1/r^2$ density profile. The system is viewed from angle i to the axis. Right: Wavelength variation of the relative contribution of each component to total flux. Note the fast change from scattering to emission dominance around 2μm. This transition is responsible for the observed wavelength variation of the image asymmetry in the near-IR.

structure, we adopted the approach of the *minimum number of free parameters* in which the bipolar cones radially extend to $R_{\rm cone}$ with the half-opening angle $\theta_{\rm cone}$. Thus our model should be considered only a first-order approximation to the actual structure of IRC+10011.

The radiative transfer calculation was performed with LELUYA, a 2D code that can handle arbitrary axially symmetric dust configurations without approximations (www.leluya.org). General scaling properties of the radiatively heated dust (Ivezić & Elitzur 1997) have been applied such that the dust condensation temperature of 900 K is the only dimensional quantity specified. All other properties can be expressed in dimensionless terms. Luminosity is irrelevant, only the stellar spectral shape is needed, which we take as black-body at 2,250 K. Similarly, only the spectral shapes of the dust absorption and scattering coefficients are needed. We use the silicate grains of Ossenkopf, Henning & Mathis (1992) with the standard size distribution described by Mathis, Rumpl & Nordsieck (1977). However, we found that fits of the visibility curves require the upper limit on the grain sizes reduced to 0.20 μm from the standard 0.25 μm.

The best fit to the overall spectral energy distribution and imaging visibility curves yields visual optical depth of 20 along the conical symmetry axis and 40 in the equatorial plane. The angular radius of the dust condensation cavity is $\sim$ 35 mas (23 $\pm$ 5 AU). The fit also yields a bolometric flux of $10^{-9}\,{\rm W/m^2}$, corresponding to 10.82 mas for the stellar angular size. The system is observed at an inclination $i = 25^\circ \pm 3^\circ$ from the axis so that the wind obscures the receding part of the bipolar structure, creating the observed asymmetry of the scattering image. When imaged at long wavelengths, such as the K'-band, the dust thermal emission starts to dominate (Figure 2, right). The asymmetry

is then less apparent since the central heating by the star tends to produce spherical isotherms.

Assuming standard gas-to-dust ratio, the overall mass of the IRC+10011 circumstellar shell is $0.13 M_\odot$. The measured wind velocity of 20 km s^{-1} gives a lifetime of $\sim$ 3,800 years for the current outflow phase. This corresponds to a mass loss rate of $3\times10^{-5} M_\odot yr^{-1}$, which is a signature of the very end of AGB evolution. Our modeling suggests the existence of a toroidal density enhancement at distances of more than $\sim$ 100 AU. Imaging observation by Marengo et al. (1999) provide a possible indication of such structure.

2.2. Bipolar cones as expanding jet cocoons

The derived gas density at the base of each cone is $1.3\times10^{6} cm^{-3}$, while at the base of the wind region it is $1.7\times10^{8} cm^{-3}$. This large disparity implies that the bipolar cones are sustained by high-velocity ram pressure, most probably due to high-velocity low-density jets. We find that the opening angle of the cones is $2\theta_{\rm cone} = 30^\circ$ and they extend to about 500 to 1000 AU. The cone emission comes from the swept-up ambient wind material. All of these properties are consistent with the jet evolution picture first described by Scheuer (1974): jets are clearing the polar regions but are trapped by the ambient material pushed ahead by their ram pressure, resulting in an expanding cocoon. The current density distribution in the cocoon is just a snapshot of an inherently dynamic structure. We find the jet lifetime is $\sim$ 200 years. In comparison with the other asymmetric AGB objects, IRC+10011 currently provides the youngest known example of asymmetry in AGB outflows.

References

Bergman, P., Kerschbaum, F., & Olofsson, H. 2000, A&A, 353, 257

Biller, B. A., et al. "Asymmetric Planetary Nebulae III", Mt. Rainier National Park, 28 July - 1 August 2003

Elitzur, M., Goldreich, P., & Scoville, N. 1976, ApJ, 205, 384

Goldreich, P., & Scoville, N. 1976, ApJ, 205, 144

Haniff, C. A., & Buscher, D. F. 1998, A&A, 334, L5

Hofmann K.-H., et al. 2001, A&A, 379, 529 (H01)

Imai, H., et al. 2002, NATURE, 417, 829

Ivezić, Ž, & Elitzur, M. 1997, MNRAS, 287, 799

Kahane, C., et al. 1997, ApSS, 251, 223

Lindqvist, M., et al. 2000, A&A, 361, 1036

Kahane, C., Jura, M. 1996, A&A, 310, 952

Marengo M., et al. 1999, A&A, 348, 501

Mathis, J. S., Rumpl, W., Nordsieck, K. H. 1977, ApJ, 217, 425

Miranda, L. F., et al. 2001, NATURE, 414, 284

Monnier, J. D., Tuthill, P. G., & Danchi, W. C. 2000, ApJ, 545, 957

Ossenkopf, V., Henning, Th., Mathis, J. S. 1992, A&A, 261, 567

Osterbart, R., et al. 2000, A&A, 357, 169

Plez, B., Lambert, D. L. 1994, ApJ, 425, L101
Riera, A., et al. 2003, A&A, 401, 1039
Scheuer, P. A. G. 1974, MNRAS, 166, 513
Schmidt, G. D., Hines, D. C., & Swift, S. 2002, ApJ, 576, 429
Sahai, R. 2002, RevMexAA, 13, 133
Sahai, R., & Trauger, J. T. 1998, AJ, 116, 1357
Sahai, R., et al. 1999, ApJ, 514, L115
Sahai, R., et al. 2003, ApJ, 586, L81
Sahai, R., et al. 2003, NATURE, *in press*
Scheuer P. A. G. 1974, MNRAS, 166, 513
Skinner, C. J., Meixner, M., & Bobrowsky, M. 1998, MNRAS, 300, L29
Su, K. Y. L., Hrivnak B. J., & Kwok S. 2001, AJ, 122, 1525
Weigelt, G., et al. 1998, A&A, 333, L51
Weigelt, G., et al. 2002, A&A, 392, 131